Phase Shifters vs Switches

Phase Shifters vs Switches: An Energy Efficiency Perspective on Hybrid Beamforming

Sohail Payami, Naveen Mysore Balasubramanya, Christos Masouros*, Mathini Sellathurai

***Abstract*—Hybrid beamforming architectures provide promising solutions to harness the benefits of massive multi-input multi-output (MIMO) systems by incorporating phase shifters, switches or their combinations. This letter addresses the design of such architectures from an energy efficiency (EE) perspective. We provide closed-form expressions to compare several promising hybrid beamforming architectures, and also derive optimal numbers of antennas required for maximizing the EE. Our results indicate that the asymptotic closed-forms provide a good approximation even for relatively small number of antennas. Moreover, the combination of phase shifters and switches offers significantly higher EE against conventional PS-only architectures, while nearly preserving spectral efficiency.**

***Index Terms*—Massive MIMO, hybrid beamforming, phase shifter selection**

I. Introduction

Hybrid analog-and-digital beamformers have attracted a lot of attention as an enabling technique to reduce the cost and power consumption of massive multiple-input multiple-output (MIMO) systems [1]. In hybrid beamforming (HB), a small number of radio frequency (RF) chains are connected to a large number of antennas through a network of analog components such as switches and/or phase shifters. Generally, switches consume lesser power than phase shifters, but using a switch-only network results in much lower spectral efficiency (SE) than a phase shifter (PS)-only network [2].

The SE and energy efficiency (EE) aspects of HB with a PS-only network have been thoroughly investigated in [1]–[7]. For instance, the impact of the insertion losses of the PSs on SE and EE is evaluated in [3]. A comprehensive study of EE for PS-only or switch-only HB can be found in [4]–[7].

Recently, we proposed new architectures for HB where a combination of phase shifters and switches are used [8], [9]. Focusing on uncorrelated independent and identically distributed (i.i.d.) Rayleigh fading channel model, we introduced a PS selection technique which allows for turning off 50% of the phase shifters without an impact on SE [8]. Based on the idea of PS selection, we designed new structures to significantly reduce the number of the phase shifters by using a simple switch network while the SE is almost preserved [9]. Simulation results in [9] indicated that the proposed PS selection techniques are also effective for correlated Rayleigh fading and sparse scattering channels. However, [8], [9] only considered the SE perspective of HB with PSs and switches, the following questions remain unanswered: 1) What is the energy efficiency behavior of different hybrid beamforming structures with PSs and switches? 2) Which HB structure is the most energy efficient method? 3) What is optimum number of antennas to achieve the maximum EE?

With this motivation, we present the EE performance of HB when different combinations of phase shifters and switches are used. In addition, we provide the closed-form expressions for EE based on the asymptotic results obtained for SE in [8], [9]. This allows for gaining simultaneous insights into both the EE and SE behaviors for each structure; which can be used as a design guide in selecting the suitable HB architectures according to the desired criteria. We also derive a near-optimal number of base station (BS) antennas that is required to maximize the EE (denoted by N^*). Simulation results demonstrate that our asymptotic closed-form expressions for EE and N^* can be still used to evaluate the EE behavior of HB systems, even when the number of antennas is relatively small.

The work is supported by the UK EPSRC grant EP/M014126/1, Large Scale Antenna Systems Made Practical: Advanced Signal Processing for Compact Deployments. S. Payami, N. M. Balasubramanya and M. Sellathurai are with Heriot-Watt University, UK (emails: {s.payami, nm81, m.sellathurai}@hw.ac.uk). C. Masouros is with University College London (email: c.masouros@ucl.ac.uk).

II. System Model and Background

Consider a single-cell multiuser massive MIMO downlink scenario where the BS has N omni-directional antennas and it serves $K \ll N$ single-antenna users. BS applies $\mathbf{F} \in \mathcal{C}^{N\times K}$ to precode the vector of modulated symbols $\mathbf{u} \in \mathcal{C}^{K\times 1}$ with $\mathrm{E}[\mathbf{u}\mathbf{u}^{\mathrm{H}}] = \mathbf{I}_K$. The channel input vector is $\mathbf{x} = (\sqrt{P/\Gamma})\mathbf{F}\mathbf{u}$ where $\Gamma = \mathrm{trace}(\mathbf{F}\mathbf{F}^H)/K$ is normalization factor such that the average transmit power per modulated symbol is P. The received signal vector $\mathbf{y} \in \mathcal{C}^{K\times 1}$ becomes

$$\mathbf{y} = \sqrt{P/\Gamma}\mathbf{H}\mathbf{F}\mathbf{u} + \mathbf{z}, \tag{1}$$

where $\mathbf{H}$ and $\mathbf{z}$ represent channel matrix and noise vector, respectively. It is assumed that the wireless channel matrix $\mathbf{H} \in \mathcal{C}^{K\times N}$ is available at the BS and the K single-antenna users cannot collaborate. Moreover, the channel coefficients $h_{k,n}$ follow frequency-flat, uncorrelated and i.i.d. Rayleigh fading model according to $h_{k,n} \sim \mathcal{CN}(0,1)$, $\forall k \in \{1, ..., K\}$ and $\forall n \in \{1, ..., N\}$. The normalized noise vector $\mathbf{z} \in \mathcal{C}^{K\times 1}$ is i.i.d. additive white Gaussian noise vector according to $z_k \sim \mathcal{CN}(0, 1/\rho)$. For the simplicity of notation, ρ is normalized such that it includes the effects of total transmit power, channel large scale fading factor and noise, i.e. it is a measure of SNR without including the transmitter array gain.

Let B and R_{sum} denote the system bandwidth and achievable sum-rate, respectively. Then, the EE is defined as

$$E = BR_{\text{sum}}/P_{\text{tot}}, \tag{2}$$

where P_{tot} represents total power that is required to achieve R_{sum}. We model P_{tot} as $P_{\text{tot}} = P_{\text{c}} + P_{\text{var}}$, [3], where P_{c} is the common power consumption term and P_{var} is the variable term for the beamforming structures. Specifically, $P_{\text{c}} = P/\eta + P_{\text{syn}}$

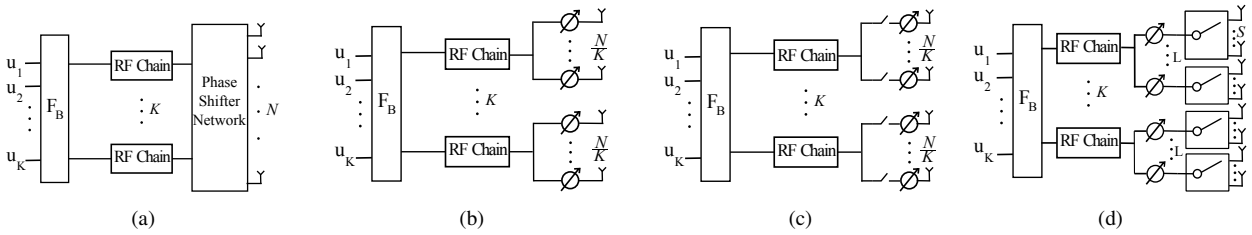

Fig. 1. a) Fully-connected, b) subconnected, c) subconnected with PSS, d) subconnected with reduced number of PSs.

where η is the efficiency of the power amplifier and P_{syn} is the power consumption of the frequency synthesizer, respectively. On the other hand, P_{var} depends on the RF circuitry according to $P_{\text{var}} = N_{\text{RF}}P_{\text{RF}} + N_{\text{PS}}P_{\text{PS}} + N_{\text{S}}P_{\text{S}}$ where N_{RF}, N_{PS}, N_{S}, P_{RF}, P_{PS} and P_{S} represent the number and the power consumption of the RF chains, phase shifters and switches, respectively.

For massive MIMO systems, digital zero-forcing (DZF) is known to be an asymptotically optimal precoder that maximizes the SE when $\mathbf{H}$ follows uncorrelated i.i.d. Rayleigh fading. In this case, the achievable sum-rate is $R_{\text{sum}}^{\text{DZF}} = K\log_2(1+\rho(N-K))$ [8]. The system requires N RF chains and the EE of the fully digital system becomes

$$E^{\text{DZF}} = BK\log_2(1+\rho(N-K))/(P_{\text{c}} + NP_{\text{RF}}). \quad (3)$$

III. EE of Hybrid Precoders with PS selection

In this section, we present our contributions in terms of introducing the EE model and deriving closed-form approximations of EE for the HB structures in Fig. 1. We also provide of the asymptotic closed-form expression of sum-rate when PS selection technique is applied to multiuser scenario with fully-connected HB. Moreover, we derive the approximations of the optimum number of BS antennas for the structures shown Fig. 1. In the following, it is assumed that $K = N_{\text{RF}}$ as it maximizes the spatial multiplexing gain at reasonably high signal-to-noise ratio (SNR) [8].

Traditional fully-connected PS-only (FP): Figure 1(a) presents the block diagram of a fully-connected PS-only HB structure where the antennas and RF chains are connected through a network of phase shifters. The precoding matrix $\mathbf{F}^{\text{FP}}$ is factorized into RF beamformer and digital precoding matrices according to $\mathbf{F}^{\text{FP}} = \mathbf{F}_{\text{RF}}^{\text{FP}}\mathbf{F}_{\text{B}}^{\text{FP}}$, where $\mathbf{F}_{\text{RF}}^{\text{FP}} \in \mathcal{C}^{N\times K}$ and $\mathbf{F}_{\text{B}}^{\text{FP}} \in \mathcal{C}^{K\times K}$. Let $\mathbf{H} = \mathbf{U}\mathbf{\Sigma}\mathbf{V}^{\text{H}}$ denote the singular value decomposition (SVD) of $\mathbf{H}$ where $\mathbf{\Sigma} \in \mathcal{R}^{K\times N}$ is diagonal matrix of singular values and $\mathbf{V} \in \mathcal{C}^{N\times N}$ and $\mathbf{U} \in \mathcal{C}^{K\times K}$ contain the right and left singular vectors. In [8], it was shown that $f_{\text{RF},n,k}^{\text{FP}} = 1/\sqrt{N}\text{e}(j\angle v_{n,k})$ and $\mathbf{F}_{\text{B}}^{\text{FP}} = (\mathbf{H}\mathbf{F}_{\text{RF}}^{\text{FP}})^{-1}$ is an asymptotically optimal solution to maximize the sum-rate. If the transmit power P is fixed, then EE is maximized when the sum-rate is maximum. Hence, the same set of beamforming matrices will maximize the EE. In Fig. 1(a), there are $N_{\text{PS}} = N_{\text{RF}}N = KN$ phase shifters and the EE of this structure is

$$E^{\text{FP}} \approx \frac{BK\log_2(1+\pi\rho(N-K)/4)}{P_{\text{c}} + KP_{\text{RF}} + KNP_{\text{PS}}}. \quad (4)$$

Remark: Although the numerator in (4) represents the *asymptotic* SE by the proposed beamformer, it provides a good approximations of performance in the nonasymptotic regime [8]. SE expressions with similar nonasymptotic behavior for the other structures are available in [9].

Fully-connected with PS selection (FPSS): The aim of PS selection is to identify and turn off the phase shifters that have negligible impact on SE. This approach was first introduced in [8] for point-to-point HB with fully-connected structure, and later it was applied to a multiuser scenario with subconnected hybrid precoder in [9]. This structure is realized equipping each PS in Fig. 1(a) with an ON/OFF switch to protect the phase shifters when they are turned off. Similar to the previous approach, the RF beamformer is set as

$$f_{\text{RF},n,k}^{\text{FPSS}} = \begin{cases} 0 & \text{if } \sqrt{N}|v_{n,k}| \le \alpha, \\ \exp(j\angle v_{n,k}) & \text{if } \alpha < \sqrt{N}|v_{n,k}|. \end{cases} \quad (5)$$

where α a threshold level to turn off the phase shifters. For uncorrelated i.i.d. Rayleigh fading channels, (5) results in switching off approximately $\beta\% = 1-\exp(-\alpha^2)$ of the phase shifters [8].

Lemma. When the RF beamformer and the baseband precoder in Fig. 1(a) are set according to (5) and $\mathbf{F}_{\text{B}}^{\text{FPSS}} = (\mathbf{H}\mathbf{F}_{\text{RF}}^{\text{FPSS}})^{-1}$, the total sum-rate $R_{\text{sum}}^{\text{FPSS}}$, for $N \to \infty$ and uncorrelated i.i.d. Rayleigh fading, is expressed as $R_{\text{sum}}^{\text{FPSS}} = K\log_2(1+\gamma)$ where

$$\gamma = \frac{\rho(N-K)\left(\frac{\sqrt{\pi}}{2} + \alpha\text{e}^{-\alpha^2} - \frac{\sqrt{\pi}}{2}\text{erf}(\alpha)\right)^2}{(1-\beta/100)}. \quad (6)$$

Proof: Considering Appendix F of [8] and section IV of [9], the proof is straightforward. □

In this structure, there are $N_{\text{S}} = KN$ switches that are always active and $\lfloor(1-\beta/100)NK\rfloor$ phase shifters that are in operation. For the sake of notation simplicity, we assume β is chosen carefully such that $(1-\beta/100)NK$ is an integer. Hence, the floor function can be removed. The EE of the Fig 1(a) when PS selection is applied becomes

$$E^{\text{FPSS}} \approx \frac{BK\log_2\left(1 + \frac{\rho(N-K)\left(\frac{\sqrt{\pi}}{2}+\alpha\text{e}^{-\alpha^2} - \frac{\sqrt{\pi}}{2}\text{erf}(\alpha)\right)^2}{(1-\beta/100)}\right)}{P_{\text{c}} + KP_{\text{RF}} + (1-\beta/100)KNP_{\text{PS}} + KNP_{\text{S}}}. \quad (7)$$

Subconnected PS-only (SP): Although the fully-connected structure of Fig. 1(a) can nearly achieve the performance of digital beamformers, it requires a complex circuitry and a large number of phase shifters. In addition, the power consumption of fully-connected structures can be very high due to the large number of phase shifters. Such structures also suffer from high levels of crosstalk distortion due to the large number of RF routes. Hence, the HB of Fig. 1(b) with subconnected structure, where each RF chain connected to a subset of antennas, is preferred in practice. The closed-form expressions

A_i^q \ q	FPSS	SPSS	SRPS
A_1^q	$1-\frac{\rho K(\frac{\sqrt{\pi}}{2}+\alpha \mathrm{e}^{-\alpha^2}-\frac{\sqrt{\pi}}{2}\mathrm{erf}(\alpha))^2}{(1-\beta/100)}$	$1-\frac{\rho(\frac{\sqrt{\pi}}{2}+\alpha \mathrm{e}^{-\alpha^2}-\frac{\sqrt{\pi}}{2}\mathrm{erf}(\alpha))^2}{(1-\beta/100)}$	$1-\left(\sum_{s=0}^{S-1}\binom{S-1}{s}\frac{(-1)^s}{(s+1)^{3/2}}\right)^2 S\rho\pi/4$
A_2^q	$\frac{\rho(\frac{\sqrt{\pi}}{2}+\alpha \mathrm{e}^{-\alpha^2}-\frac{\sqrt{\pi}}{2}\mathrm{erf}(\alpha))^2}{(1-\beta/100)}$	$\frac{\rho(\frac{\sqrt{\pi}}{2}+\alpha \mathrm{e}^{-\alpha^2}-\frac{\sqrt{\pi}}{2}\mathrm{erf}(\alpha))^2}{K(1-\beta/100)}$	$\left(\sum_{s=0}^{S-1}\binom{S-1}{s}\frac{(-1)^s}{(s+1)^{3/2}}\right)^2 S\rho\pi/4K$
A_3^q	$P_{\mathrm{c}}+KP_{\mathrm{RF}}$	$P_{\mathrm{c}}+KP_{\mathrm{RF}}$	$P_{\mathrm{c}}+KP_{\mathrm{RF}}$
A_4^q	$(1-\beta/100)KP_{\mathrm{PS}}+KP_{\mathrm{S}}$	$(1-\beta/100)P_{\mathrm{PS}}+P_{\mathrm{S}}$	$P_{\mathrm{PS}}/S+P_{\mathrm{S}}$

TABLE I. Values of A_i^q, $\forall i \in \{1,...,4\}$, $q \in \{\text{FPSS, SPSS, SRPS}\}$ in (12)-(16).

of an asymptotically optimal PS-only HB for subconnected structure and its sum-rate $R_{\text{sum}}^{\text{SP}}$ was derived in [9]. It offers hardware simplicity at the cost of lower SE. Figure 1(b) only requires N phase shifters and K RF chains. Hence, the EE of subconnected structure in Fig. 1(b) is approximated by

$$E^{\text{SP}} \approx \frac{BK\log_2\left(1+\frac{\pi\rho(N-K)}{4K}\right)}{P_{\mathrm{c}}+KP_{\mathrm{RF}}+NP_{\mathrm{PS}}} \tag{8}$$

Compared to (4) for the fully-connected PS-only HB structure, the sum-rate (numerator of (8)) has a factor of $1/K$ inside the logarithm which represents smaller array gain. However, the power consumption (denominator) is reduced by $(K-1)NP_{\mathrm{PS}}$ (linear scale), indicating a possible improvement in the EE.

Subconnected with PS selection (SPSS): In order to apply PS selection to the subconnected structure of Fig. 1(b), we equip each PS with a dedicated switch as shown in Fig. 1(c). In this method, the number of the required phase shifters and switches is equal to N. However, the number of the active phase shifters is reduced to $N(1-\beta/100)$ compared to Fig. 1(b). In this case, the EE is approximated by

$$E^{\text{SPSS}} \approx \frac{BK\log_2\left(1+\frac{\rho(N-K)\left(\frac{\sqrt{\pi}}{2}+\alpha \mathrm{e}^{-\alpha^2}-\frac{\sqrt{\pi}}{2}\mathrm{erf}(\alpha)\right)^2}{K(1-\beta/100)}\right)}{P_{\mathrm{c}}+KP_{\mathrm{RF}}+(1-\beta/100)NP_{\mathrm{PS}}+NP_{\mathrm{S}}}. \tag{9}$$

Subconnected with reduced number of phase shifters and PS selection (SRPS): Recently in [9], we proposed the architecture of Fig. 1(d) where simple 1-out-S switches, e.g. binary switches, are used to reduce the number of phase shifters to N/S. As shown in Fig. 1(d), each PS can be connected to only one of the S adjacent antennas. The aim of this structure is to allow for adding extra low cost antennas to an existing system and benefit from the favorable conditions of massive MIMO systems. For the sake of simplicity, we use an equivalent model where the 1-out-of-S is replaced with a combination of a splitter and S ON/OFF switches. The final result is same as having one switch per antenna. Figure 1(d) consists of K RF chains, $L=N/SK$ phase shifters and N switches and its EE is approximated by

$$E^{\text{SRPS}} \approx \frac{BK\log_2\left(1+\frac{\left(\sum_{s=0}^{S-1}\binom{S-1}{s}\frac{(-1)^s}{(s+1)^{3/2}}\right)^2 S\rho\pi(N-K)}{4K}\right)}{P_{\mathrm{c}}+KP_{\mathrm{RF}}+NP_{\mathrm{PS}}/S+NP_{\mathrm{S}}}. \tag{10}$$

Optimal number of antennas: The optimal value of N for the structures in Fig. 1 is derived by solving

$$N^{\mathrm{q}^*} = \arg\max_N E^{\mathrm{q}}, \tag{11}$$

where $q \in \{\text{FPSS, SPSS, SRPS}\}$. By rearranging the expressions of E^q presented above, in terms dependent/independent of N, (11) can be written in the general form

$$N^{\mathrm{q}^*} \approx \arg\max_N \frac{BK\log_2(A_1^{\mathrm{q}}+A_2^{\mathrm{q}}N)}{A_3^{\mathrm{q}}+A_4^{\mathrm{q}}N}, \tag{12}$$

where $A_i^q, \forall i \in \{1,...,4\}$ are constant numbers and presented in Table. I. We only present the results for the PS selection based structures as the derivation of EE for other structures is straightforward. It can be noted that the numerator and denominator of (12) for all the PS selection based structures are quasi-concave and and affine functions, respectively. Hence, (12) is quasi-concave and N^{q^*} is the global maximum [10]. Differentiating the right hand side of (12) with respect to N and setting it equal to zero, we obtain

$$\frac{A_2^{\mathrm{q}}(A_3^{\mathrm{q}}+A_4^{\mathrm{q}}N)}{\ln(2)(A_1^{\mathrm{q}}+A_2^{\mathrm{q}}N)} = \frac{A_4^{\mathrm{q}}\ln(A_1^{\mathrm{q}}+A_2^{\mathrm{q}}N)}{\ln(2)}. \tag{13}$$

Let $t=\ln(A_1^{\mathrm{q}}+A_2^{\mathrm{q}}N)$, then (13) can be reorganized as

$$(t-1)\exp(t-1) = (A_2^{\mathrm{q}}A_3^{\mathrm{q}}-A_1^{\mathrm{q}}A_4^{\mathrm{q}})/eA_4^{\mathrm{q}}, \tag{14}$$

where e is Euler's constant. Using Lambert function W (which is defined as the inverse function of $x \mapsto xe^x$ [11]), we get

$$(t-1) = W\left((A_2^{\mathrm{q}}A_3^{\mathrm{q}}-A_1^{\mathrm{q}}A_4^{\mathrm{q}})/eA_4^{\mathrm{q}}\right). \tag{15}$$

Considering that $N=(\exp(t-1)-A_1^{\mathrm{q}})/A_2^{\mathrm{q}}$ may not result in an integer number, the approximate close-form for N^{q^*} can be expressed as

$$N^{\mathrm{q}^*} \approx \left\lfloor \left(e^{W\left(\frac{A_2^{\mathrm{q}}A_3^{\mathrm{q}}-A_1^{\mathrm{q}}A_4^{\mathrm{q}}}{eA_4^{\mathrm{q}}}\right)+1}-A_1^{\mathrm{q}}\right)/A_2^{\mathrm{q}} \right\rfloor. \tag{16}$$

It is noted that for the subconnected structure further rounding might be required to obtain integer N^{q^*}.

IV. Simulation Results

In this section, Monte Carlo simulations over 1000 channel realizations are used to provide a comparison between the SE and EE of HB structures shown in Fig. 1. The closed-form approximations of the SE of the proposed methods can be deduced from the numerator of EE formulas in this manuscript. Similar to [3], we set $\eta = 0.39$, $P_{\mathrm{RF}} = 1$ W, $P_{\mathrm{Syn}} = 2$ W and $B = 20$ MHz. The power consumption of each of the phase shifters P_{PS} and switches P_{S} at 2.4 GHz are reported as $28.8 \le P_{\mathrm{PS}} \le 152$ mW [12] and $0 < P_{\mathrm{S}} \le 15$ mW [13]. In the following, we use $P_{\mathrm{PS}} = 30$ mW, $P_{\mathrm{S}} = 1$ mW, $\rho = 10$ dB, $P = 10$ W and $K = 4$. It could be

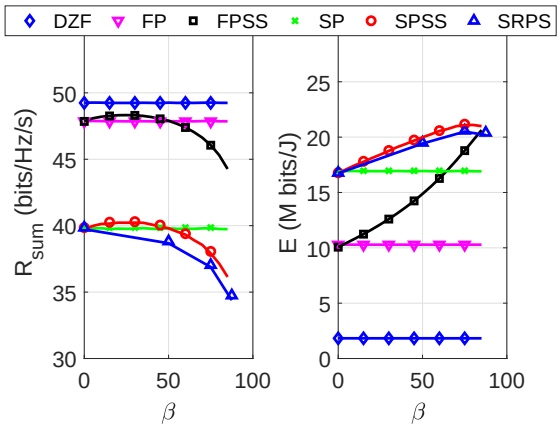

Fig. 2. SE (left) and EE (right) vs β. Solid lines and markers present simulation and close-forms, respectively.

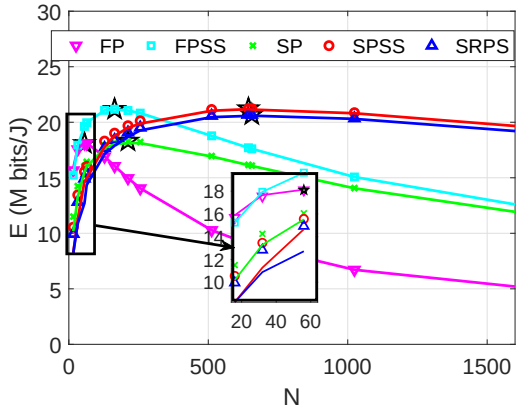

Fig. 3. EE vs N. Solid lines and markers present simulation and close-forms, respectively. Five-pointed stars show N^{q^*} in (16).

easily verified that setting $S \in \{1, 2, 4, 8\}$ is equivalent to $\beta \in \{0\%, 50\%, 75\%, 87.5\%\}$.

Setting $N = 512$, Fig. 2 presents the SE and EE results for different values of β. Evidently, there is a good match between the simulation results and the closed-form approximations of SE and EE. Compared to PS-only network, Fig. 2 shows that PS selection achieves a competitive SE even when 75% of the phase shifters are deactivated. Fully-digital system provides the highest SE, but it has the lowest EE compared to other methods. Amongst the hybrid structures, traditional HB with fully-connected PS-only network has the best spectral and worst energy efficiencies. When PS selection with $\beta = 75\%$ is applied to fully-connected beamformer, it provides around 80% higher EE while $R_{\text{sum}}^{\text{FPSS}}$ is only around 1.8 bits/Hz/s lower than $R_{\text{sum}}^{\text{FP}}$. At $\beta = 75\%$, it is observed that E^{SPSS} and E^{SRPS} are comparable with each other, however, $R_{\text{sum}}^{\text{SPSS}}$ is slightly higher than $R_{\text{sum}}^{\text{SRPS}}$. Using both structures results more than 20% better EE compared to E^{SP} while they achieve more than 95% of the achievable sum-rates (around 1.8 bits/Hz/s loss).

Setting $S = 4$, $\beta = 75\%$ and $16 \leq N < 1600$, Fig. 3 depicts N^{q^*} and EE vs N behavior for different HB structures. It is observed that the closed-forms (shown with markers) provide a better approximation of EE with respect to the simulations (solid lines), as N increases $\forall N \geq 64$. Moreover, PS selection based techniques significantly improve the EE compared to the PS-only counterparts. The optimum value for the number of antennas and its corresponding EE for each structure (stars in Fig. 3) are calculated by inserting N^{q^*} from (16) into (4), (7), (8), (9) and (10). Compared to the simulations (maximum of the solid curves), our presented closed-forms provide a good approximation for the optimum operation point. The results in this section imply that the presented formulas can be used as a guide to evaluate the EE performance of hybrid beamformers even in the nonasymptotic regimes.

V. Conclusion

In this letter, we showed that applying PS selection for massive MIMO hybrid beamforming can significantly increase the energy efficiency while the spectral efficiency is almost preserved. The energy efficiency gains are more noticeable for fully-connected hybrid beamformers. It was shown that turning off 75% of the phase shifters has minimal impact on the sum-rates but it almost doubles the energy efficiency. The promising performance of the subconnected structure with reduced number of phase shifters, makes it a cost-effective method to realize the benefits of massive MIMO systems.

References

[1] O. El Ayach, S. Rajagopal, S. Abu-Surra, Z. Pi, and R. Heath, "Spatially sparse precoding in millimeter wave MIMO systems," *IEEE Trans. Wireless Commun.*, vol. 13, no. 3, pp. 1499–1513, March 2014.

[2] X. Zhang, A. Molisch, and S.-Y. Kung, "Variable-phase-shift-based RF-baseband codesign for MIMO antenna selection," *IEEE Trans. Signal Process.*, vol. 53, no. 11, pp. 4091–4103, November 2005.

[3] A. Garcia-Rodriguez, V. Venkateswaran, P. Rulikowski, and C. Masouros, "Hybrid analog-digital precoding revisited under realistic RF modeling," *IEEE Wireless Commun. Lett.*, vol. 5, no. 5, pp. 528–531, Oct 2016.

[4] X. Gao, L. Dai, S. Han, C. L. I, and R. W. Heath, "Energy-efficient hybrid analog and digital precoding for MmWave MIMO systems with large antenna arrays," *IEEE J. Sel. Areas Commun.*, vol. 34, no. 4, pp. 998–1009, April 2016.

[5] C. G. Tsinos, S. Maleki, S. Chatzinotas, and B. Ottersten, "On the energy-efficiency of hybrid analog-digital transceivers for single- and multi-carrier large antenna array systems," *IEEE J. Sel. Areas Commun.*, vol. 35, no. 9, pp. 1980–1995, Sept 2017.

[6] R. Mendez-Rial, C. Rusu, N. Gonzalez-Prelcic, A. Alkhateeb, and R. W. Heath, "Hybrid MIMO architectures for millimeter wave communications: Phase shifters or switches?" *IEEE Access*, vol. 4, pp. 247–267, 2016.

[7] R. Mendez-Rial, C. Rusu, A. Alkhateeb, N. Gonzalez-Prelcic, and R. W. Heath, "Channel estimation and hybrid combining for mmwave: Phase shifters or switches?" *Info. Theory and Appl. Wkshp. (ITA), 2015*, pp. 90–97, February 2015.

[8] S. Payami, M. Ghoraishi, and M. Dianati, "Hybrid beamforming for large antenna arrays with phase shifter selection," *IEEE Trans. Wireless Commun.*, vol. 15, no. 11, pp. 7258–7271, Nov 2016.

[9] S. Payami, M. Ghoraishi, M. Dianati, and M. Sellathurai, "Hybrid beamforming with reduced number of phase shifters for massive MIMO systems," *IEEE Trans. Veh. Technol.*, 2018.

[10] S. Boyd and L. Vandenberghe, *Convex Optimization*. New York, NY, USA: Cambridge University Press, 2004.

[11] R. M. Corless, G. H. Gonnet, D. E. G. Hare, D. J. Jeffrey, and D. E. Knuth, "On the lambertw function," *Advances in Computational Mathematics*, vol. 5, no. 1, pp. 329–359, Dec 1996. [Online]. Available: https://doi.org/10.1007/BF02124750

[12] Y. Zheng and C. E. Saavedra, "An ultra-compact CMOS variable phase shifter for 2.4-GHz ISM applications," *IEEE Trans. Microw. Theory Techn.*, vol. 56, no. 6, pp. 1349–1354, June 2008.

[13] N. A. Talwalkar, C. P. Yue, H. Gan, and S. S. Wong, "Integrated CMOS transmit-receive switch using LC-tuned substrate bias for 2.4-GHz and 5.2-GHz applications," *IEEE J. Solid-State Circuits*, vol. 39, no. 6, pp. 863–870, June 2004.